Journal of Cell Science 107, 2191-2202 (1994)
Printed in Great Britain © The Company of Biologists Limited 1994

Replication factories and nuclear bodies: the ultrastructural characterization of replication sites during the cell cycle

Pavel Hozák[1,2], Dean A. Jackson[1] and Peter R. Cook[1,*]

[1]CRC Nuclear Structure and Function Research Group, Sir William Dunn School of Pathology, University of Oxford, South Parks Road, Oxford OX1 3RE, UK
[2]Institute of Experimental Medicine, Academy of Sciences of the Czech Republic, Vídeňská 1083, 142 20 Prague 4, Czech Republic

*Author for correspondence

SUMMARY

Sites of replication in synchronized HeLa cells were visualized by light and electron microscopy; cells were permeabilized and incubated with biotin-16-dUTP, and incorporation sites were immunolabelled. Electron microscopy of thick resinless sections from which ~90% chromatin had been removed showed that most DNA synthesis occurs in specific dense structures (replication factories) attached to a diffuse nucleoskeleton. These factories appear at the end of G_1-phase and quickly become active; as S-phase progresses, they increase in size and decrease in number like sites of incorporation seen by light microscopy. Electron microscopy of conventional thin sections proved that these factories are a subset of nuclear bodies; they changed in the same characteristic way and contained DNA polymerase α and proliferating cell nuclear antigen. As replication factories can be observed and labelled in non-permeabilized cells, they cannot be aggregation artifacts. Some replication occurs outside factories at discrete sites on the diffuse skeleton; it becomes significant by mid S-phase and later becomes concentrated beneath the lamina.

Key words: cell nucleus, ultrastructure, nuclear body, nucleoskeleton, replication factory

INTRODUCTION

Various sub-compartments within nuclei have recently been characterized (e.g. see Saunders et al., 1991; Lamond and Carmo-Fonseca, 1993), including several different types of 'nuclear bodies' (for reviews, see Bouteille et al., 1974; Ascoli and Maul, 1991; Brasch and Ochs, 1992). These electron-dense structures are seen in conventional thin sections, but their functional role remains obscure. Whilst characterizing replication sites, we found that these sites corresponded to a sub-set of nuclear bodies.

Replication sites are not diffusely spread throughout nuclei but concentrated in discrete regions. For example, early in S-phase ~150 foci can be seen by fluorescence microscopy after incubating rat fibroblasts with bromodeoxyuridine and immunolabelling sites of incorporation; later during S-phase the foci are fewer in number and larger (Nakamura et al., 1986; Nakayasu and Berezney, 1989). Analogous foci can be labelled after incubating permeabilized mammalian cells or demembranated frog sperm in egg extracts in the presence of biotin-dUTP (e.g. see Mills et al., 1989; Hozák et al., 1993; see also O'Keefe et al., 1992).

The ultrastructural characterization of replication sites poses several problems. [^{3}H]thymidine incorporated by living cells can be localized autoradiographically, but the path-length of β-particles is too long to allow precise localization. Synthetic sites can also be immunolabelled after incubation with bromodeoxyuridine (e.g. see Mazzotti et al., 1990; O'Keefe et al., 1992). However, DNA synthesis occurs so rapidly in vivo (i.e. at ~1500 nucleotides or 0.5 μm/min) that during incubations sufficient to allow subsequent detection, nascent DNA can move far from its synthetic site. Whilst synthetic rates can be reduced using permeabilized cells, the non-physiological buffers often used may artifactually aggregate nascent DNA and polymerases on to underlying structures (Cook, 1988; Martelli et al., 1990).

We minimize these problems by encapsulating living HeLa cells in agarose microbeads (diameter ~25-150 μm), before permeabilizing cell membranes with streptolysin O (Ahnert-Higler et al., 1989) in a 'physiological' buffer. Under optimal conditions, such permeabilized cells synthesize DNA at the in vivo rate (Jackson et al., 1988); if complexes containing polymerases had aggregated artifactually, they should lose activity. Such permeabilized cells incorporate biotin-dUTP into foci that can be subsequently immunolabelled with fluorescent tags; these cannot be fixation artifacts because similar foci are found in unfixed cells (Hassan and Cook, 1993). Encapsulation protects fragile cells and allows thorough washing to remove endogenous pools of triphosphates and unbound antibodies; then the use of low precursor concentrations ensures that only synthetic sites are labelled. Encapsulation also allows both structure and function to be preserved during lengthy manipu-

lations. For example, after cutting the chromatin fibre with nucleases and electrophoretic removal of most obscuring chromatin, a diffuse nucleoskeleton can be seen in thick (resinless) sections (Jackson and Cook, 1988); essentially all polymerizing activity and nascent DNA remain associated with residual nuclear structures (Jackson and Cook, 1986a,b).

Earlier, we used this approach to immunolocalize sites of replication in early S-phase cells using thick (resinless) sections, which allow the visualization of three-dimensional structures (Hozák et al., 1993). Chromatin-depleted nuclei contain a diffuse nucleoskeleton associated with residual chromatin. Ovoid bodies, which had roughly the same size and number as fluorescent foci at the same stage of the cycle, were attached to this skeleton. Immunolabelling after incorporation of biotin-dUTP showed that these ovoids were sites of replication. As each ovoid must contain ~20 replication forks, we called them replication 'factories'. We now extend this study to other stages of interphase and confirm that replication takes place in a sub-set of nuclear bodies.

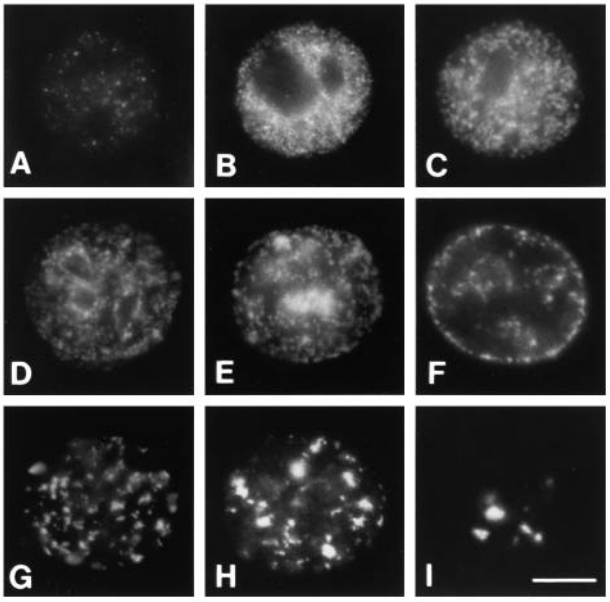

Fig. 1. Fluorescence micrographs of replication patterns found in cells at different stages of the cycle. Cells (8, 10, 12, 14, 14, 14, 16.5, 16.5 and 18 hours post-mitosis for A-I, respectively) were encapsulated, permeabilized and incubated with biotin-dUTP, and sites of incorporation were indirectly immunolabelled. Bar, 5 μm.

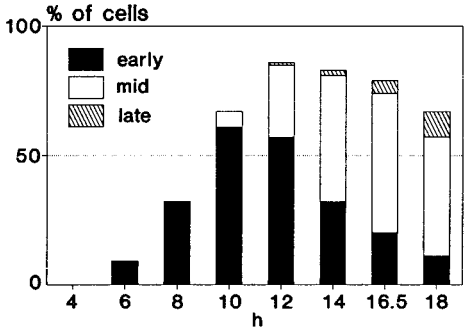

Fig. 2. Changing replication patterns during the cell cycle. The percentages of cells with early, mid and late patterns illustrated in Fig. 1A-C, D-F and G-I were determined at the times indicated; 200 cells from 3-5 experiments were counted at each time.

MATERIALS AND METHODS

Cell culture and synchronization

Suspension cultures of HeLa cells were grown in minimal essential medium supplemented with 10% foetal calf serum. They were then synchronized using thymidine and nitrous oxide (Jackson and Cook, 1986b): cells were blocked in S-phase (2.5 mM thymidine; 22 hours), washed carefully, regrown for 4 hours in fresh medium, arrested in mitosis using nitrous oxide at high pressure (8 hours; >98% in mitosis) and regrown (sometimes up to 10% remain blocked in mitosis). Samples were taken at 4 hours (G_1), 6 and 8 hours (G_1/S border), 10 hours (early S), 14 hours (mid S), 16.5 hours (late S), and 18 hours (late S/G_2).

Encapsulation and lysis

Cells were washed in PBS and in some cases were encapsulated (1×10^6 to 10×10^6 cells/ml) in 0.5% agarose. Encapsulated or unencapsulated cells were incubated with streptolysin O (Murex; 1.5 i.u./ml per 10^6 cells; 30 minutes; 4˚C), washed with ice-cold PBS to remove unbound streptolysin and then a modified 'physiological' buffer (PB; Jackson et al., 1988). PB (pH 7.4) contains 22 mM Na^+, 130 mM K^+, 1 mM Mg^{2+}, <0.3 μM free Ca^{2+}, 67 mM Cl^-, 65 mM CH_3COO^-, 11 mM phosphate, 1 mM ATP, 1 mM dithiothreitol and 0.1 mM phenylmethylsulphonyl fluoride (PMSF). Beads or cells were resuspended in 10 vol. PB and immediately permeabilized by incubation (37˚C; 2 minutes).

Replication in vitro

A prewarmed replication mix (10× concentrate) was added to lysed cells (whether encapsulated or not) to give final concentrations of 100 μM CTP, UTP and GTP, 250 μM dCTP, dATP and dGTP, plus 100 μM biotin-16-dUTP (Boehringer) and 2.15 mM $MgCl_2$ (1 mM ATP and 1 mM $MgCl_2$ are present in PB). After 5 or 30 minutes (for electron microscopy and immunofluorescence, respectively) at 33˚C, reactions were stopped with 10 vol. ice-cold PB.

Immunofluorescence

After stopping replication in vitro, encapsulated cells were washed in 0.2% Triton in PB (10 minutes; 0˚C) to permeabilize nuclear membranes, washed 3× in PB, fixed (15 minutes; 4˚C) in fresh 4% paraformaldehyde in PB, washed 4× in PBS, incubated (4 hours; 20˚C) with primary antibody (goat anti-biotin; 2.5 μg/ml; Sigma) in PBS supplemented with 0.05% bovine serum albumin and 0.1% Tween 20, washed 4× in PBS + supplements, incubated (16 hours; 4˚C) with secondary antibody (donkey anti-goat; 2.5 μg/ml; Jackson Laboratories), washed 4× in PBS + supplements and the beads were mounted under coverslips in Vectashield (Vector Labs). Photographs were taken using a Zeiss Axiophot microscope and Kodak T-max black and white film.

Chromatin digestion and electroelution

After stopping replication in vitro, encapsulated cells were pelleted, incubated (20 vol.; 2× 5 minutes; 0˚C) in 0.2% Triton in PB to permeabilize nuclei, washed 4× in ice-cold PB, incubated (20 minutes; 33˚C) with *Eco*RI (2500 units/ml) and *Hae*III (500 units/ml) in PB and then subjected to electrophoresis (0.8% agarose gel; 4 V/cm; 3.5 hours, 4˚C) in PB supplemented with PMSF. The nuclease treatment cuts chromatin into ~10 kb pieces (*Eco*RI cuts a *Hae*III-resistant satellite) and electroelution routinely removes ~90% chromatin as measured by removal of ^3H after pre-labelling living cells with [^3H]thymidine (Jackson et al., 1990).

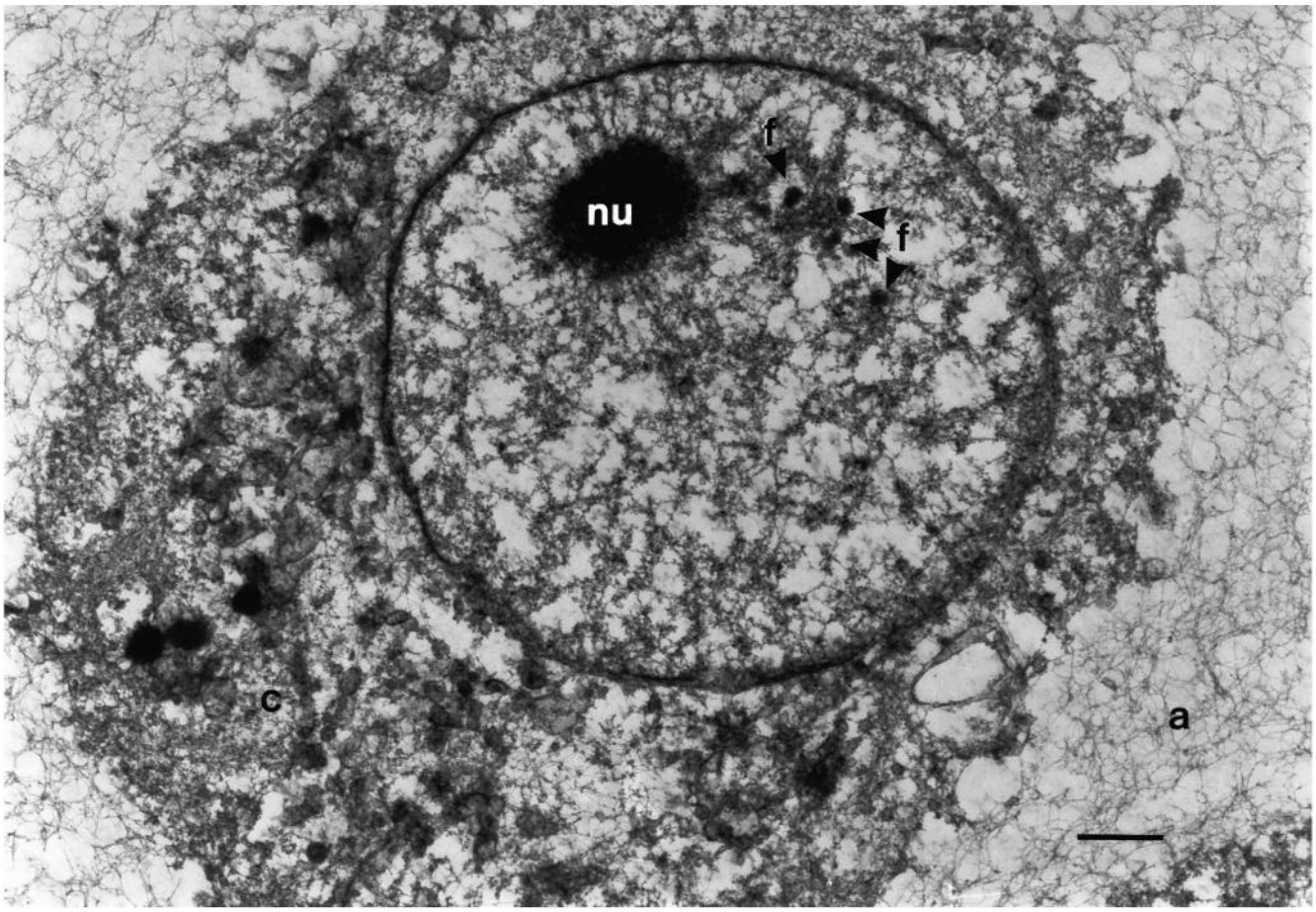

Fig. 3. Electron micrograph of cell 10 hours post-mitosis from which ~90% chromatin has been removed. Encapsulated cells were permeabilized, incubated with biotin-dUTP and treated with nucleases; chromatin was eluted, incorporated biotin immunolabelled with 5 nm gold particles, and a 500 nm resinless section was prepared. Agarose (a) surrounds cytoplasmic (c) and nuclear remnants where residual clumps of chromatin are attached to a diffuse network that ramifies from nucleolus (nu) to lamina. Gold particles, which are not visible at this magnification, were concentrated in replication factories (f). Bar, 1 μm.

Pre-embedding immunoelectron microscopy

Encapsulated and eluted cells were fixed (10 minutes; 0˚C) with 0.5% glutaraldehyde in PB, washed 2× in 0.1 M Na/K phosphate Sörensen buffer (pH 7.4; SB), incubated (10 minutes) in 0.02 M glycine in SB, and rewashed in SB. After incubation (20 minutes; 20˚C) with 5% normal rabbit serum, cells were incubated (1 hour; 20˚C) with goat anti-biotin antibody (5 μg/ml; Sigma) in TBT buffer (20 mM Tris, 150 mM NaCl, 0.1% bovine serum albumin, 0.005% Tween 20, 20 mM Na_3N; pH 8.2), washed 3× in TBT and incubated (1 hour) with rabbit anti-goat antibody conjugated with 5 nm gold particles (50× dilution in TBT + 0.5% fish gelatine; BioCell). After washing 2× in TBT and once in SB, cells were fixed (20 minutes) in 2.5% glutaraldehyde in SB, washed 3× in SB, postfixed with 0.5% OsO_4 in SB, dehydrated through an ethanol series (including 30 minutes of incubation in 2% uranyl acetate in 70% ethanol), and embedded in Araldite epoxy-resin for conventional electron microscopy. Ultrathin sections were contrasted with uranyl acetate and lead citrate according to Reynolds. For resinless sections, the ethanol was replaced in three steps by *n*-butanol. Samples were then embedded in the removable compound diethylene glycol distearate (DGD; Polysciences) and resinless sections were prepared (Fey et al., 1986; Hozák et al., 1993): beads were immersed in a DGD/*n*-butanol mixture at 60˚C, impregnated with pure DGD, blocks were hardened, and 500 nm thick sections were cut using a diamond knife and placed onto Pioloform-coated grids (Agar; grids preincubated with poly-L-lysine in water), DGD was removed (3× 1.5 hours incubations in *n*-butanol; 20˚C), butanol replaced by acetone, and specimens were critical-point dried. Sections were observed in Jeol JEM 100CX electron microscope (accelerating voltage 80 kV). Quantitative data were obtained from 50 random resinless nuclear sections for each cell cycle stage studied. The best-preserved sections were obtained when: (i) beads were pelleted slowly; (ii) all solutions (made using diethylpyrocarbonate-treated water) contained PMSF and placental ribonuclease inhibitor (Amersham) at final concentrations of 25, 2.5 and 0.25 units/ml during incubations with antibodies, subsequent washes and electroelution, respectively; and (iii) samples were critical-point dried, taking care that they were free of water (Ris, 1985).

Postembedding immunoelectron microscopy

After stopping replication in vitro, unencapsulated cells were pelleted and immediately fixed (20 minutes; 0˚C) in 3% paraformaldehyde and 0.1% glutaraldehyde in PB. After washing in SB (including 10 minutes of incubation in 0.02 M glycine in SB), cells were dehydrated in ice-cold ethanol, embedded in LR White (polymerization, 24 hours at 50˚C) and ultrathin sections on gilded copper grids were immunolabelled. Unspecific binding was blocked by preincubation (30 minutes) with an appropriate 10% pre-immune serum in PBS with 0.1% Tween-20 and 1% BSA (PBTB buffer), sections were incubated (40 minutes) with primary antibodies (1-5 μg/ml) in PBTB, washed in PBS, incubated (40 minutes) with gold-conjugated secondary

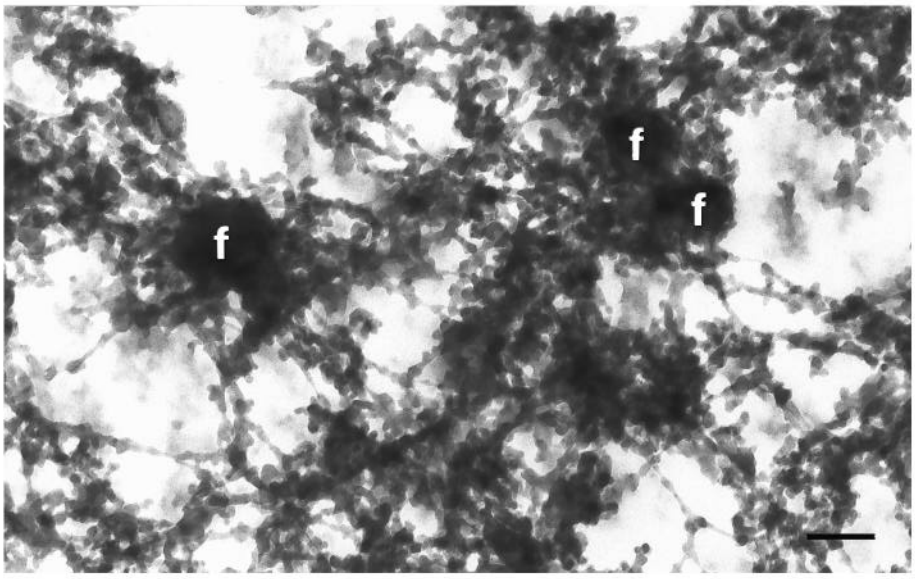

Fig. 4. As Fig. 3, but the cell is 8 hours post-mitosis. Three structures (factories; f) are associated with a diffuse skeleton. A background level of gold particles is distributed throughout the field. Bar, 200 nm.

antibody in PBTB (pH 8.2), rewashed and contrasted with a saturated solution of uranyl acetate in water. Primary antibodies used included goat anti-biotin (Sigma) and a monoclonal anti-PCNA (proliferating cell nuclear antigen) antibody, PC-10 (Oncogene Science); 5 or 10 nm gold-conjugated antibodies included rabbit anti-goat (Sigma), goat anti-mouse (BioCell), or goat anti-biotin (BioCell).

Electron microscopy of intact cells

Synchronized cells were washed in SB, fixed immediately without permeabilization, embedded in epoxy resin or LR White and immunolabelled as above.

RESULTS

Immunofluorescence

We first characterized synthetic sites by immunofluorescence. More than 95% HeLa cells were blocked in mitosis and after releasing the block the first cells enter S-phase 5.5 hours later; DNA synthesis then peaks 10 hours after mitosis before the last cells leave S-phase 18 hours post-mitosis (see Jackson and Cook, 1986b, for an illustration of the quality of synchrony). Cells at different stages were encapsulated, lysed with streptolysin, incubated for 30 minutes with biotin-16-dUTP to allow elongation of nascent DNA chains by ~3000 nucleotides, and sites of biotin incorporation were indirectly immunolabelled (Hozák et al., 1993; Hassan and Cook, 1993). Despite the excellent synchrony at mitosis, each time-point inevitably contains a mixture of cells at different stages of the cycle; even so, it was obvious that the pattern of fluorescent foci changed, as indicated in the typical examples shown in Fig. 1. As these are photographs of round nuclei, many foci lie above or below the focal plane and generate a background 'flare'. Incorporated label is removed by DNase treatment (Hozák et al., 1993; Hassan and Cook, 1993).

Replication begins in small foci spread throughout extranucleolar regions (Fig. 1A). They become brighter, larger and more numerous (Fig. 1B,C), before they aggregate (Fig. 1D,E) to become concentrated around nucleoli and the nuclear periphery (Fig. 1F) in mid S-phase. Later, they become more central, larger and fewer in number (Fig. 1G-I). These patterns illustrate arbitrarily chosen points along a continuum and are typical of patterns seen by others (e.g. see Nakamura et al., 1986; Nakayasu and Berezney, 1989; Kill et al., 1991; Humbert and Usson, 1992). Given that ~3000 replication forks are active at any one time, even the smallest foci must contain >20 replication forks.

This sequence was confirmed by measuring the percentage of cells with each pattern at different times; early, middle and late patterns (i.e. Fig. 1A-C, D-F and G-I, respectively) peaked after 10, 16.5 and 18 hours, respectively (Fig. 2).

Replication factories in the cell cycle

We next characterized replication sites by electron microscopy of thick resinless sections; permeabilized cells were incubated with biotin-dUTP for 5 minutes, ~90% chromatin removed and sites containing incorporated biotin immunolabelled with 5 nm gold particles. Under these conditions, nascent chains are extended by ~500 nucleotides and essentially all remain within nuclei despite removal of most chromatin (Hozák et al., 1993).

Fig. 5. As Fig. 3 (cell 10 hours post-mitosis). (A) There are 77 gold particles in this field, which are not visible at this magnification; 58% were in factories (f) attached to a diffuse skeleton (d), which is connected to core filaments (c) and the lamina (l). Bar, 0.5 μm. (B) High-power view of arrowed factory in A. Arrowheads indicate some gold particles that are difficult to see against the dense background. Bar, 100 nm. (C) Higher magnification and underexposure of lower half of factory in B. Arrowheads indicate the same gold particles arrowed in B. Bar, 50 nm.

Fig. 6. As Fig. 3, but the cell is 14 hours post-mitosis. (A) Clusters of labelled factories (f) and unlabelled dense factories (df) surround a nucleolus (nu) and a fibrous network (arrowed); 28, 10 and 21% of the 70 nuclear gold particles, which are not visible at this magnification, were in factories, dense factories and extra-factory clusters on the skeleton, respectively. l, lamina. Arrow indicates area enlarged in B. Bar, 0.5 μm. (B) Enlargement of arrowed region in A. Arrowheads indicate some gold particles in two labelled factories (f). df, unlabelled dense factory. Bar, 100 nm. (C,D) Enlargements and underexposures of labelled factories (f) in B; arrowheads indicate the same gold particles as in B. Bar, 50 nm.

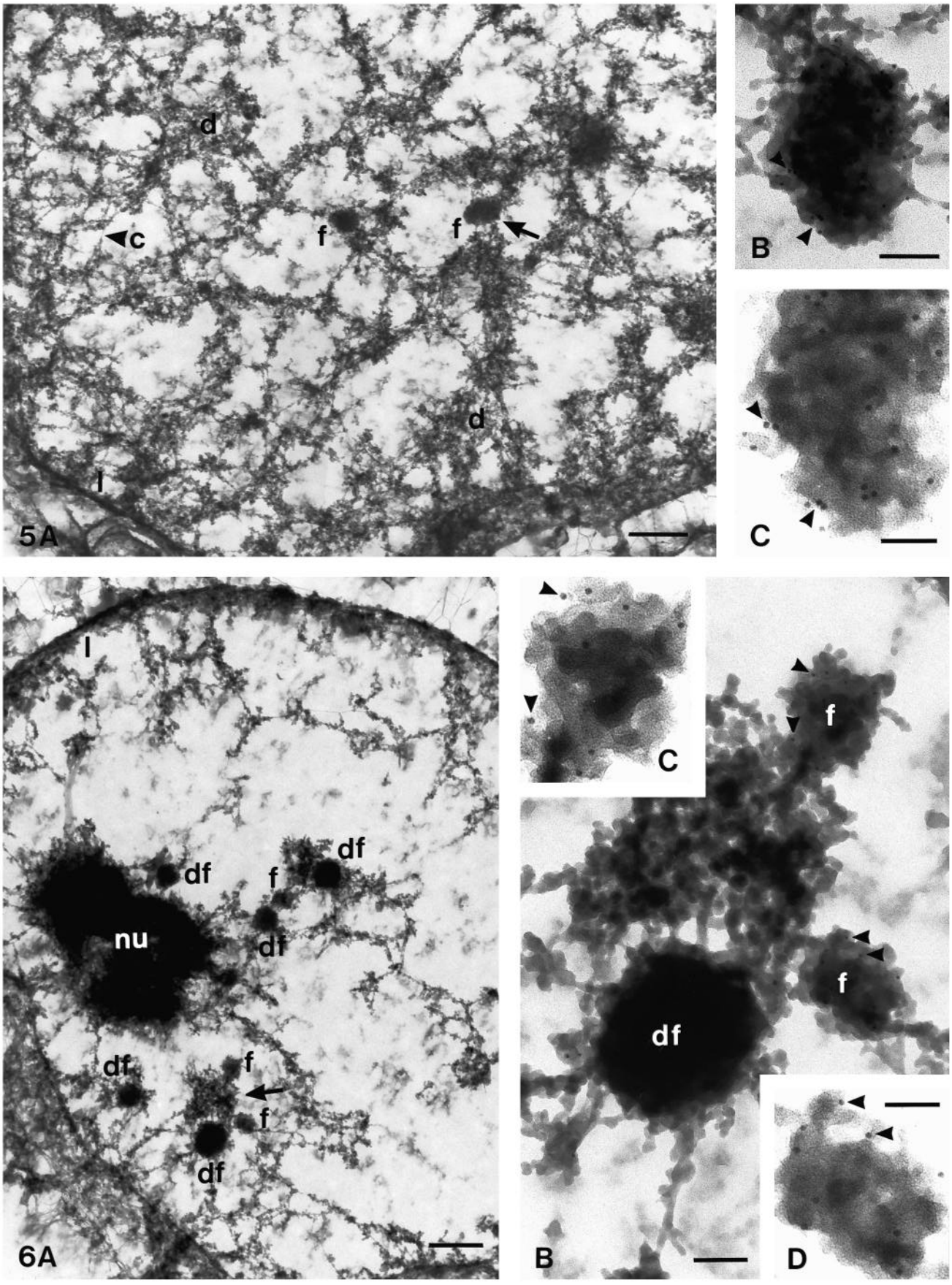
d
c
f
f
d
l
5A
B
C
l
df
df
f
nu
df
df
f
f
df
6A
C
f
f
df
B
D

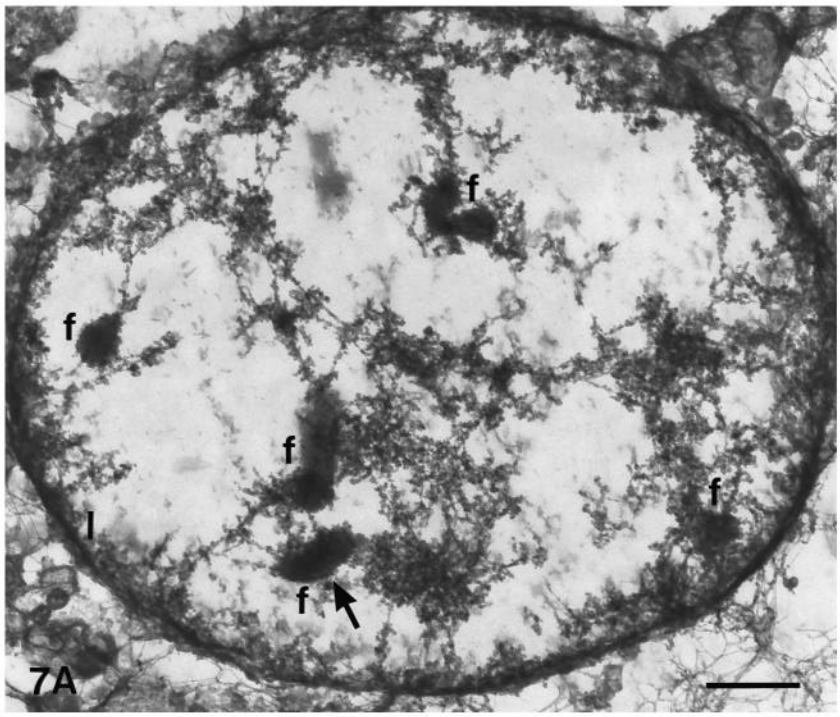
f
f
f
f
f
l
7A

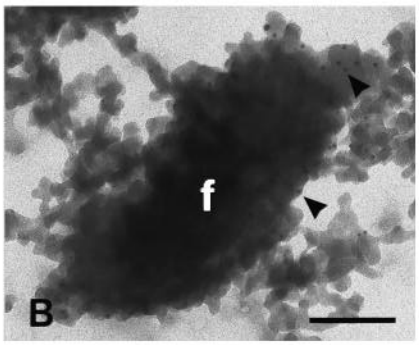
f
B

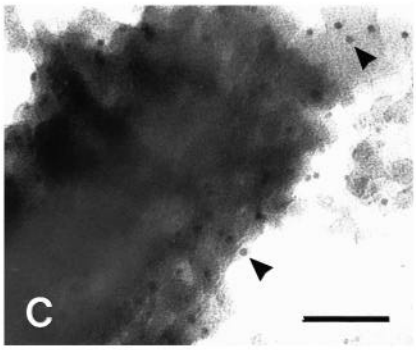
C

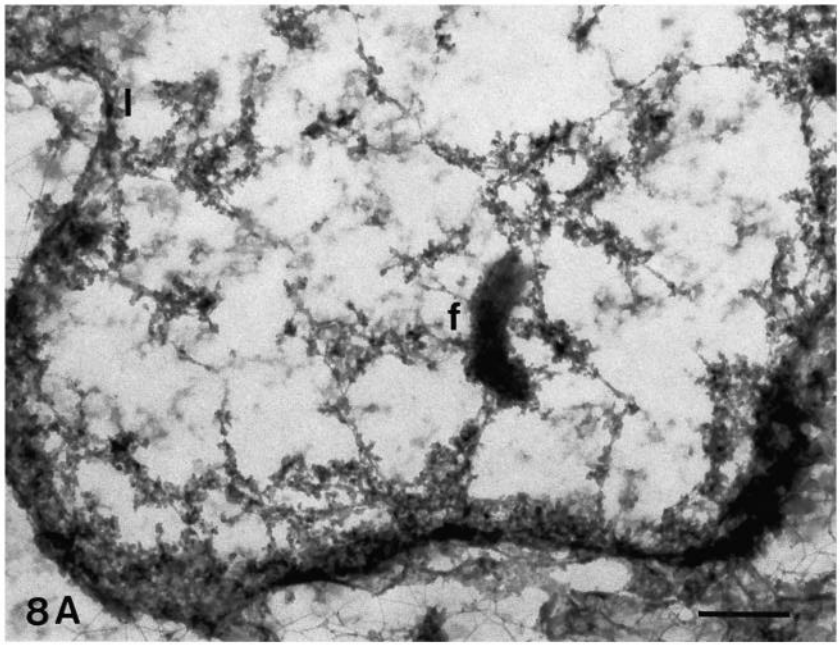
l
f
8A

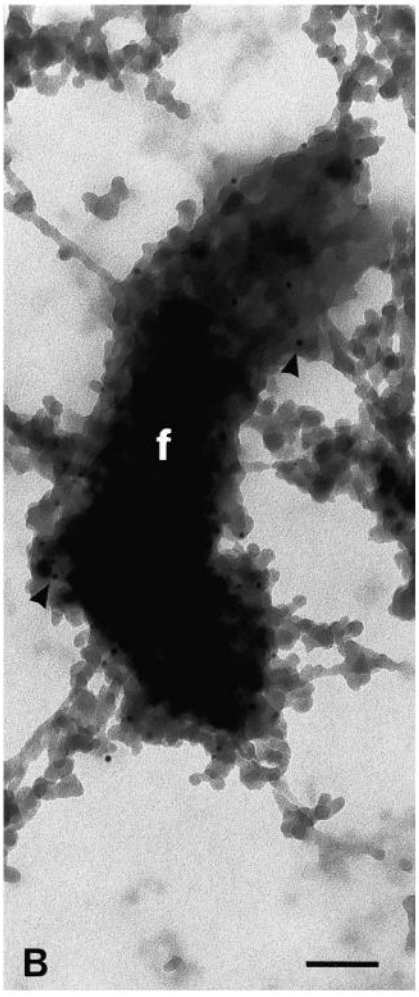
f
B

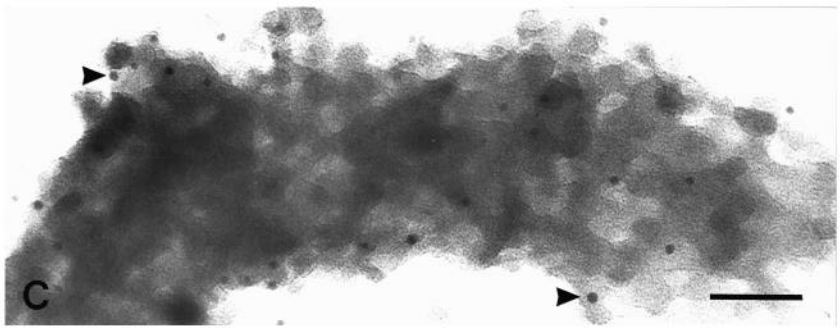
C

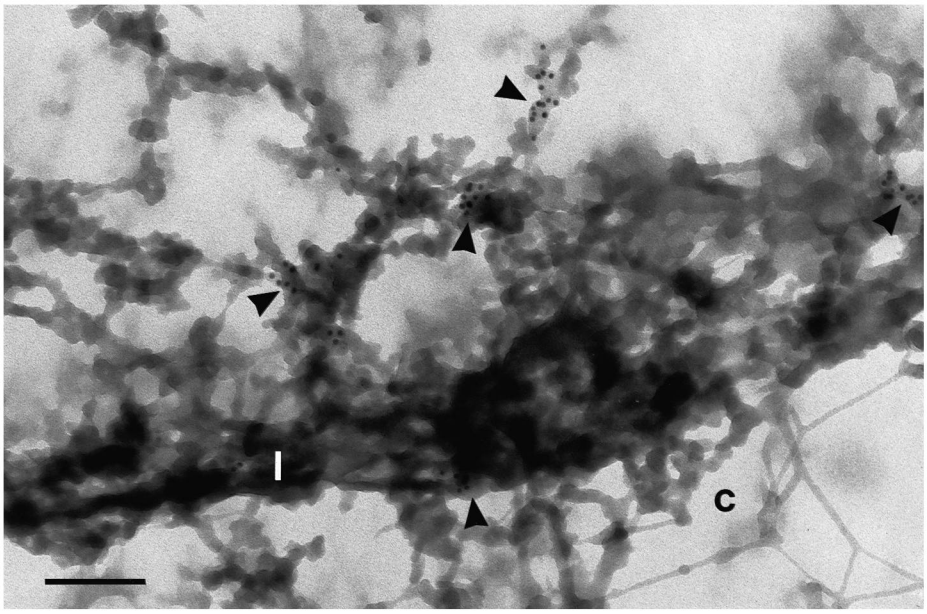

Fig. 9. As Fig. 3, but cell 16.5 hours post-mitosis. 93% of the 53 particles in the field were in 5 extra-factory clusters (arrowheads). c, cytoplasm. l, lamina. Bar, 100 nm.

In a typical low-power view of an early S-phase cell (Fig. 3), agarose filaments (a) surround the remains of the cytoplasm (c) and within the nuclear region, ovoid replication factories (f) are attached to a diffuse skeleton.

G_1 cells contain up to four (unlabelled) dense structures like the factories in Fig. 3. At the G_1/S border, the numbers of these structures increases rapidly (see below) to equal the number of fluorescent foci at the same stage (e.g. Fig. 1B). They are initially unlabelled (Fig. 4), but soon become labelled and contain most gold particles in the section (Hozák et al., 1993, have analyzed this time-point in detail).

By mid S-phase, factories become rounder, larger - with a long axis of 250-400 nm - and not so diffusely spread, just like fluorescent foci (compare Fig. 5A with Fig. 1D). In the medium-power view of Fig. 5A, the skeletal network is seen to be composed of core filaments (c) covered by diffuse elements (d). As before, label is concentrated in these mid-sized factories (Fig. 5B,C).

Fig. 6 illustrates factories clustered around nucleoli and the nuclear periphery, like fluorescent foci in Fig. 1E,F. A significant fraction of these medium-sized factories are very dense, round and poorly labelled (Fig. 6A, df), often close to a region rich in diffuse skeleton. Later in S-phase (and again like their fluorescent counterparts) factories are more internal and often bi- or tri-lobed, as if they had arisen by fusion of smaller, rounder structures (Fig. 7) in a process reminiscent of the fusion of prenucleolar bodies during nucleologenesis (reviewed by Fischer et al., 1991). Finally, they become very large (i.e. up to 700 nm long) and frequently sausage-like; they are almost always labelled (Fig. 8).

Fig. 7. As Fig. 3, but the cell is 16.5 hours post-mitosis. (A) 72 and 12% of the 429 particles in the field were in the factories (f) and extra-factory clusters on the skeleton, respectively. l, lamina. Arrow indicates factory enlarged in B. Bar, 0.5 μm. (B) Enlargement of arrowed factory in A. Arrowheads mark gold particles. Bar, 100 nm. (C) Enlargement and underexposure of top of factory in B; arrowheads indicate the same gold particles arrowed in B. Bar, 50 nm.

Fig. 8. As Fig. 3, but the cell is 18 hours post-mitosis. (A) 60 and 14% of the 85 particles in the field were in the large factory (f) and extra-factory clusters on the skeleton, respectively. l, lamina. Bar, 0.5 μm. (B) Enlargement of factory in A. Arrowheads mark gold particles. Bar, 100 nm. (C) Enlargement and underexposure of middle of factory in B; arrowheads indicate the same gold particles arrowed in B. Bar, 50 nm.

Extra-factory labelling

Although label is concentrated in factories throughout S-phase, some is found outside factories in focal regions on the diffuse skeleton. Initially, a few foci are scattered throughout nuclei, usually where many elements of the diffuse skeleton are concentrated. Such scattered extra-factory labelling only becomes significant during mid S-phase and later the foci become concentrated under the lamina (Fig. 9).

The life-cycle of factories

These results could suggest that small factories grow progressively into medium-sized factories and ultimately into large factories. Although difficult to prove formally, a detailed analysis of 50 nuclear sections at each time-point supports such a transition (Fig. 10). At the different times, values for the percentage of labelled sections (i.e. containing at least 1 factory with at least 2 gold particles) mirrored the percentage of cells with fluorescent foci (Fig. 2). Factories were classified according to size - small, medium and large (i.e. with long axes of <250, 250-400 and >400 nm, respectively). Small factories appeared first, to be followed by medium and large factories (Fig. 10A); the percentage of each kind of structure that was labelled roughly followed the same pattern (Fig. 10B). Many mid-sized factories were clustered 14 hours post-mitosis (Fig. 10C), coincidentally with clustering seen by fluorescence microscopy (Fig. 1D-F).

Our previous study showed that factories found during early S-phase (i.e. 10.5 hours) were uniform in size (long axis 185 nm, standard deviation 45, range 120-320; Hozák et al., 1993); most of these are categorized here as ‘small’ factories. The

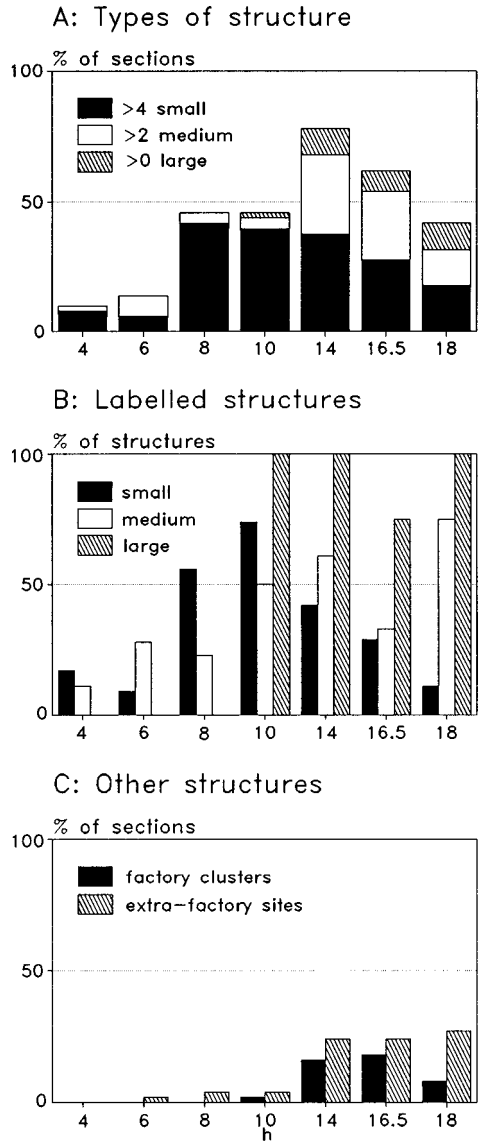

Fig. 10. The changing percentages of different structures during S-phase; 50 sections like those illustrated in Figs 3-10 were examined at each time indicated; then the percentages of sections containing small (long axis <250 nm), medium (long axis 250-400 nm) and large (long axis >400 nm) factories, factory clusters and extra-factory sites were calculated. (A) Percentage of sections with factories of different sizes (whether labelled or not). As sections from cells in G_1 and G_2 contained 0-4 small and 0-2 medium-sized structures, only sections with >4 small and >2 medium-sized structures are included in the histogram. (B) Percentage of factories of different size that were labelled with at least 2 gold particles. The total numbers of small, medium and large factories in the 50 sections at the different times were: 93, 35, 0 (4 hours); 142, 43, 0 (6 hours); 259, 43, 0 (8 hours); 174, 8, 1 (10 hours); 209, 75, 10 (14 hours); 173, 73, 4 (16.5 hours); 114, 32, 7 (18 hours), respectively. (C) Percentage of sections with factory clusters and extra-factory sites. A cluster contained >3 factories and extra-factory sites >3 gold particles.

absence of partially built (i.e. smaller) factories implies that they only become active after attaining a minimum size. If construction were lengthy, we might expect to see many unlabelled (small) factories before cells enter S-phase, but we do not (Fig. 10A, 6 hours). Moreover, when small factories first appeared in statistically significant numbers (Fig. 10A, 8 hours) <50% were unlabelled (Fig. 10B); therefore, small factories must be assembled rapidly, to become active quickly. Medium-sized factories behave similarly; when they appear in numbers (Fig. 10A, 14 hours) <50% are again unlabelled, so that they, too, must be assembled rapidly, to become active immediately. However, large factories behave differently; when they first appear in numbers none are unlabelled (Fig. 10B, 14 hours). (Only 1 unlabelled large factory was seen in the 50 sections (Fig. 10B).) This implies that they do not have to achieve full size before commissioning and are probably generated by growth and/or aggregation of smaller, active, factories.

Deconstruction of factories seems to be slower than construction. Thus, at later times, >50% small and medium-sized factories are unlabelled (Fig. 10B). We have not yet analyzed the later stages of G_2 and so do not know how long large unlabelled factories persist.

We also estimated the numbers of extra-factory replication sites - defined as a cluster of >3 particles on the diffuse skeleton. The first few clusters appeared just after the first labelled factories (Fig. 10C, 6 hours); such clusters were only seen in sections that also contained labelled factories. Significant numbers then appeared during mid S-phase (Fig. 10C, 14 hours), suggesting that extra-factory replication follows replication in factories. As labelled extra-factory sites were generally remote from factories, it seems unlikely that label had been extruded from factories.

Identification of replication factories in thin sections

The electron density of factories suggested they might be related to nuclear bodies seen in conventional thin sections. Therefore we compared labelled structures in thick and thin sections. Fig. 11A illustrates a typical view of an LR White-labelled section of an early S-phase cell; small dense bodies are labelled as shown in detail in Fig. 11B. Similar structures are seen after eluting most chromatin (Fig. 11C), which are obviously related to the factories seen in the same sample in thick sections (Fig. 11D). The dense structures in thick and thin sections changed similarly in number, size and nuclear location. For example, medium and large (labelled) structures can be seen in LR White sections from mid and late S-phase (compare Fig. 11E with Fig. 6 and Fig. 11F with Fig. 8).

In resinless sections, PCNA is concentrated in factories as well as spread over the diffuse skeleton; therefore it provides an additional marker for a factory (Hozák et al., 1993). The LR White section illustrated in Fig. 11F is doubly labelled to mark sites of biotin incorporation (10 nm particles) and PCNA (5 nm particles); the dense region is doubly labelled, confirming its identity as a factory. These results clearly identify factories as a kind of nuclear body seen in thin sections.

Ultrastructure of factories in non-permeabilized cells

It is formally possible that the labelled structures seen in both thick and thin sections are created artifactually during cell permeabilization and/or incubation. Therefore, thin sections from unlysed cells were prepared and factories identified using anti-PCNA, as unpermeabilized cells do not incorporate biotin-dUTP. At 14 hours post-mitosis, nuclear bodies in the sections

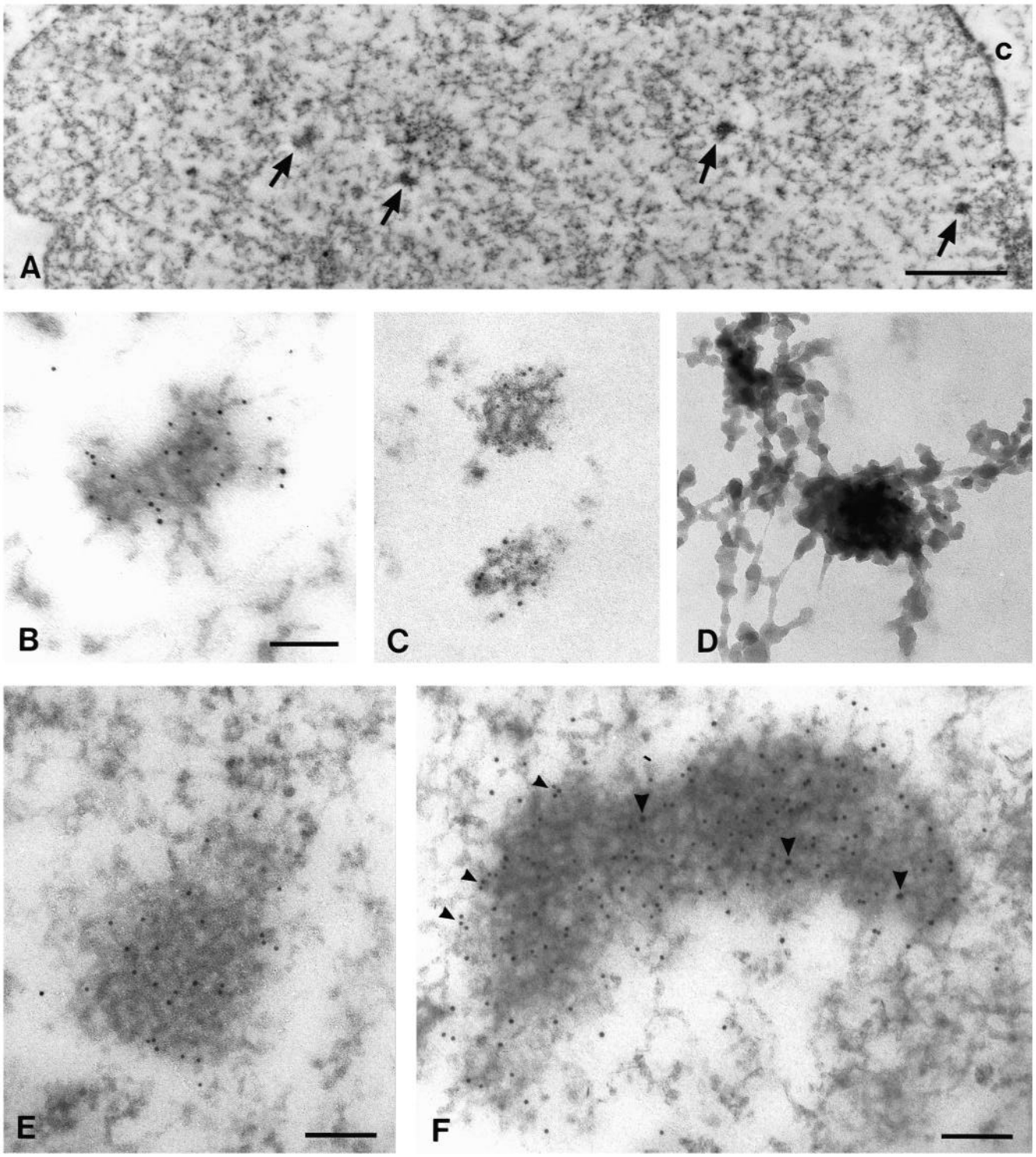

Fig. 11. Replication factories are nuclear bodies. Unencapsulated (A,B) or encapsulated (C-F) cells at various stages post-mitosis were permeabilized and incubated with biotin-dUTP; most chromatin was removed from some samples by nuclease treatment and electrophoresis (C,D) before different kinds of sections were prepared. Sites containing incorporated biotin were immunolabelled (pre- or post-embedding) with 5 (A-E) or 10 nm (F) gold particles. (A) 10 hours post-mitosis, thin (LR White) section, all chromatin present, post-embedding labelling. Most gold particles in the field, which are not visible at this magnification, were over the 4 nuclear bodies (arrowed). Bar, 1 μm. (B) An enlargement of the left-hand nuclear body in A showing gold particles. Bar, 100 nm. (C,D) 10 hours post-mitosis, thin (epoxy-resin) and thick (DGD) sections, respectively, most chromatin removed, pre-embedding labelling. Gold particles lie over factories. Magnification as B. (E) 14 hours post-mitosis, thin (LR White) section, all chromatin present, post-embedding labelling. Gold particles label the medium-sized factory. Bar: 100 nm. (F) 18 hours post-mitosis, thin (LR White) section, all chromatin present, post-embedding double-labelling. PCNA and incorporated biotin were labelled with 5 and 10 nm gold particles, respectively (some of each are labelled with small and large arrowheads); the large factory is doubly labelled. Bar, 100 nm.

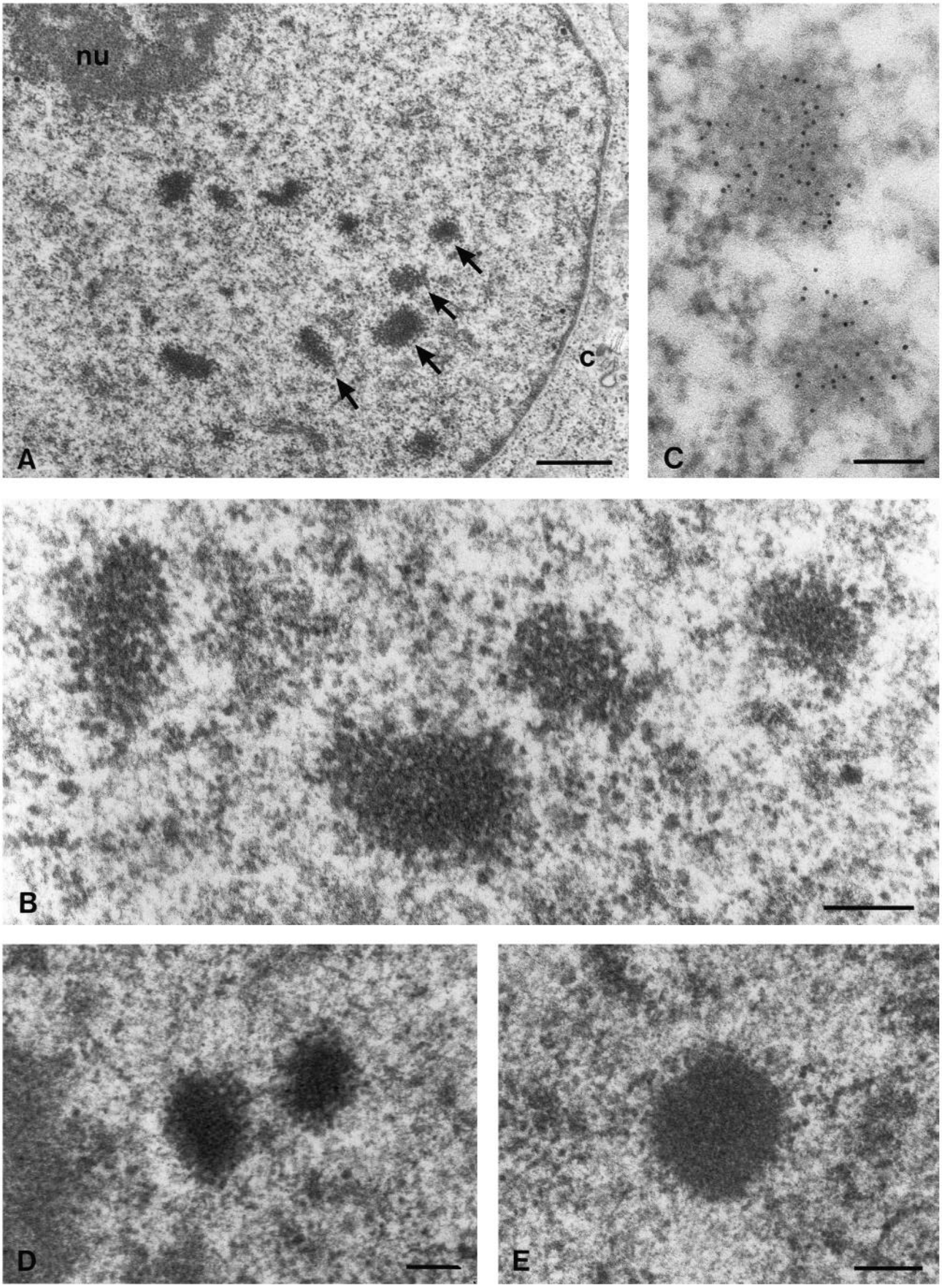
nu
c
A
C
B
D
E

(Fig. 12A) contain PCNA (Fig. 12C). Each body consists of a dense fibrillar core from which other fibres (20-25 nm diam.) radiate (Fig. 12B,D illustrates various sections). Some medium-sized bodies contain only a dense fibrillar core (Fig. 12E) and are perhaps the medium-sized dense factories seen at a comparable stage in resinless sections (Fig. 6A,B, df). Clearly, the structures in permeabilized and unpermeabilized cells are similar in number, distribution and PCNA content.

DISCUSSION

Replication factories are associated with a nucleoskeleton throughout S-phase

We have visualized sites of replication using synchronized HeLa cells encapsulated in agarose microbeads; cells were permeabilized, incubated with biotin-16-dUTP in a 'physiological' buffer and incorporation sites were immunolabelled with gold particles. Conditions were adjusted so that nascent DNA was elongated by ~500 and ~3000 nucleotides for electron and light microscopy, respectively. Electron microscopy of thick resinless sections from which ~90% chromatin had been removed showed that at all stages of S phase synthesis occurs in specific structures or 'factories' attached to a diffuse skeleton. Synthesis begins in large numbers of small factories (long axis <250 nm); in mid S-phase synthesis occurs in fewer medium-sized factories (long axis 250-400 nm) clustered around nucleoli and the nuclear periphery, whilst later a few large factories (long axis >400 nm) are found more centrally. These changes mirror those seen by immunofluorescence (Fig. 1; Nakamura et al., 1986; Nakayasu and Berezney, 1989; Kill et al., 1991; Fox et al., 1991; Humbert and Usson, 1992; Manders et al., 1992; O'Keefe et al., 1992).

During mid S-phase a small amount of extra-factory synthesis occurs at discrete sites on the diffuse skeleton (Fig. 10C); later this becomes concentrated beneath the lamina (Fig. 9). It is attractive to suppose that this extra-factory synthesis reflects the 'tidying-up' replication of unduplicated DNA left between factories.

Replication factories are nuclear bodies

Various types of 'nuclear bodies' have been seen in conventional thin sections, but no role in replication for these ill-characterized structures has yet been demonstrated (for reviews, see Bouteille et al., 1974; Ascoli and Maul, 1991; Brasch and Ochs, 1992). Our results clearly show that the factories seen in resinless sections correspond to nuclear bodies; they are similarly labelled with biotin-dUTP and PCNA and they change in number, shape and distribution in much the same way. In the absence of specific markers it is difficult to be certain which of the known nuclear bodies equates best with our factories. However, using morphological criteria, small replication factories can probably be classified as 'simple' nuclear bodies, which are known to increase in number when cells are stimulated to replicate their DNA (Brasch and Ochs, 1992). Categorization of the medium and large factories is problematic. The factories/bodies cannot be artifacts induced during permeabilization and/or incubation, since they are found in intact cells (Fig. 12).

Fig. 12. The ultrastructure of replication factories/nuclear bodies in intact cells (14 hours post-mitosis). Synchronized cells were fixed without any further treatment and embedded in epoxy resin (A,B,D,E) or LR White (C). Epoxy resin preserves ultrastructure better; LR White is best for immunolabelling. (A) Low-power view showing clusters of factories (some are arrowed) typical of mid S-phase. c, cytoplasm. nu, nucleolus. Bar, 500 nm. (B) Arrowed factories in A. Factories consist of a dense fibrillar core from which radiates 20-25 nm fibrils. Different sections have different appearances; central sections (as D) reveal both zones, apical sections (as factory on left in B) show only profiles of radiating fibrils and intermediate sections have mixed profiles (as three factories on right in B). Bar, 200 nm. (C) Densely staining region immunolabelled with anti-PCNA (5 nm gold particles); PCNA is found in replication factories. Bar, 100 nm. (D) Central sections through two factories. Bar, 200 nm. (E) Section through a dense factory; this may correspond to an unlabelled factory like those illustrated in Fig. 6A,B. Bar, 200 nm.

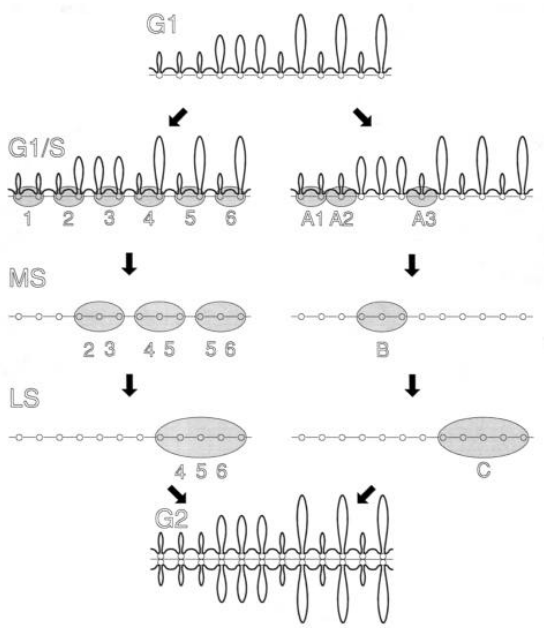

Fig. 13. Models for chromosome duplication. The G_1 chromatin fibre is shown looped by attachment to transcription factories (circles) on a skeleton (horizontal line). Small and large loops represent eu- and hetero-chromatin. For the sake of clarity, only one of the ~50 loops attached to each transcription factory during G_1, G_1/S and G_2, and none of those during mid and late S-phase (MS and LS), are shown. Most DNA is synthesized as templates slide through factories but some 'tidying-up' replication occurs outside factories to give the duplicated G_2 fibre. (See Hassan and Cook (1994), Hassan et al. (1994), Jackson and Cook (1993) and Cook (1991, 1994) for details.) Left: large factories grow from small factories. At the G_1/S border, small replication factories (shaded ovals 1-6) quickly assemble around pairs of transcription factories (generally on the same chromosome), which immediately become active. As one factory replicates many loops, not all origins need fire simultaneously. By mid S-phase, some small replication factories (e.g. 1) have become redundant; on disassembly their components are incorporated into medium-sized factories, which arise by growth and fusion (e.g. 2,3). By late S-phase, disassembly of most factories and growth/fusion of a few generates large factories (i.e. 4,5,6) which replicate most heterochromatin; they are always labelled as they grow from smaller active factories. Right: factories of different sizes are created ab initio at new sites at different times (first A1→3, then B, then C). If assembly of large factories takes time, we should see partially built, but inactive, factories (not shown).

Early autoradiographic studies suggested that [^{3}H]thymidine was incorporated into dispersed chromatin, close to variably sized masses of condensed chromatin (Bouteille et al., 1974; Fakan, 1978). As such autoradiographs provide less resolution than our micrographs, small, medium and large factories could be mistaken for chromatin clumps, especially in cells containing large amounts of heterochromatin; moreover, nascent DNA could well have moved away from its synthetic site during the longer labelling times required for autoradiography. The same is true of experiments in which synthetic sites are immunolabelled after incubating living cells for 5 minutes or more with bromodeoxyuridine (e.g. see Mazzotti et al., 1990; O'Keefe et al., 1992). Therefore these results may be consistent with ours.

Models for the duplication of the chromatin fibre

We can imagine two extreme models to explain the life cycle of factories. Small (active) factories might grow progressively and/or aggregate into larger factories (Fig. 13, left). Such a model has the advantage of simplicity, as assembly of all factories could be triggered by only one event, and it fits the morphological observations that factories grow and/or fuse as cells progress through S-phase. Alternatively, factories of different sizes might be built ab initio at different stages in different parts of the genome (Fig. 13, right), but then some mechanism must control assembly of factories of the appropriate size at the right time and place. As it probably takes time to build a large factory, we would then expect to see many partly built, but inactive, factories; however, we see few (Fig. 10B), consistent with the first alternative. In contrast, Kill et al. (1991) showed that PCNA was incorporated into fluorescent foci before they became active; their observations support the second alternative, as such foci are probably the equivalent of partly built, inactive, factories. Given the preliminary nature of these results, and the complexity of chromosome duplication, it seems prudent at this stage to assume that both alternatives apply at different stages during S-phase.

We thank Jeremy Sanderson for his help, and the Wellcome Trust (P.H. and P.R.C.) and The Cancer Research Campaign (D.A.J. and P.R.C.) for support.

REFERENCES

Ahnert-Higler, G., Mach, W., Fohr, K. J. and Gratzl, M. (1989). Poration by a α-toxin and streptolysin O: an approach to analyze intracellular processes. *Meth. Cell Biol.* **31**, 63-90.

Ascoli, C. and Maul, G. (1991). Identification of a novel nuclear domain. *J. Cell Biol.* **112**, 785-795.

Bouteille, M., Laval, M. and Dupuy-Coin A. M. (1974). Localization of nuclear functions as revealed by ultrastructural autoradiography and cytochemistry. In *The Cell Nucleus*, vol. 1 (ed. H. Busch), pp. 5-71. New York: Academic Press Inc.

Brasch, K. and Ochs R. L. (1992). Nuclear bodies (NBs): a newly 'rediscovered' organelle. *Exp. Cell Res.* **202**, 211-223.

Cook, P. R. (1988). The nucleoskeleton: artefact, passive framework or active site? *J. Cell Sci.* **90**, 1-6.

Cook, P. R. (1991). The nucleoskeleton and the topology of replication. *Cell* **66**, 627-635.

Cook, P. R. (1994). RNA polymerase: structural determinant of the chromatin loop and the chromosome. *BioEssays* **16**, 425-430.

Fakan, S. (1978). High resolution autoradiographic studies on chromatin functions. In *The Cell Nucleus*, vol. 5 (ed. H. Busch), pp 3-53. Orlando: Academic Press Inc.

Fey, E. G., Krochmalnic, G. and Penman, S. (1986). The nonchromatin substructures of the nucleus, the ribonucleoprotein (RNP)-containing and RNP-depleted matrices analyzed by sequential fractionation and resinless section microscopy. *J. Cell Biol.* **102**, 1654-1665.

Fischer, D., Weisenberger, D. and Scheer, U. (1991). Assigning functions to nucleolar structures. *Chromosoma* **101**, 133-140.

Fox, M. H., Arndt-Jovin, D. J., Jovin, T. M., Baumann, P. H. and Robert-Nicoud, M. (1991). Spatial and temporal distribution of DNA replication sites localized by immunofluorescence and confocal microscopy in mouse fibroblasts. *J. Cell Sci.* **99**, 247-253.

Hassan, A. B. and Cook, P. R. (1993). Visualization of replication sites in unfixed human cells. *J. Cell Sci.* **105**, 541-550.

Hassan, A. B. and Cook, P. R. (1994). Does transcription by RNA polymerase play a direct role in the initiation of transcription? *J. Cell Sci.* **107**, 1381-1387.

Hassan, A. B., Errington, R. J., White, N. S., Jackson, D. A. and Cook, P. R. (1994). Replication and transcription sites are colocalized in human cells. *J. Cell Sci.* **107**, 425-434.

Hozák, P., Hassan, A. B., Jackson, D. A. and Cook, P. R. (1993). Visualization of replication factories attached to a nucleoskeleton. *Cell* **73**, 361-373.

Humbert, C. and Usson, Y. (1992). Eukaryotic DNA replication is a topographically ordered process. *Cytometry* **13**, 603-614.

Jackson, D. A. and Cook, P. R. (1986a). Replication occurs at a nucleoskeleton. *EMBO J.* **5**, 1403-1410.

Jackson, D. A. and Cook, P. R. (1986b). A cell-cycle dependent DNA polymerase activity that replicates intact DNA in chromatin. *J. Mol. Biol.* **192**, 65-76.

Jackson, D. A. and Cook, P. R. (1988). Visualization of a filamentous nucleoskeleton with a 23 nm axial repeat. *EMBO J.* **7**, 3667-3677.

Jackson, D. A., Yuan, J. and Cook, P. R. (1988). A gentle method for preparing cyto- and nucleo-skeletons and associated chromatin. *J. Cell Sci.* **90**, 365-378.

Jackson, D. A., Dickinson, P. and Cook, P. R. (1990). Attachment of DNA to the nucleoskeleton of HeLa cells examined using physiological conditions. *Nucl. Acids Res.* **18**, 4385-4393.

Jackson, D. A. and Cook, P. R. (1993). Transcriptionally active minichromosomes are attached transiently in nuclei through transcription units. *J. Cell Sci.* **105**, 1143-1150.

Kill, I. R., Bridger, J. M., Campbell, K. H. S., Maldona-Codina, G. and Hutchison, C. J. (1991). The timing of the formation and usage of replicase clusters in S-phase nuclei of human diploid fibroblasts. *J. Cell Sci.* **100**, 869-876.

Lamond, A. I. and Carmo-Fonseca, M. (1993). The coiled body. *Trends Cell Biol.* **3**, 198-204.

Manders, E. M. M., Stap, J., Brakenhoff, G. J., van Driel, R. and Aten, J. A. (1992). Dynamics of three-dimensional replication patterns during the S-phase, analyzed by double labelling of DNA by confocal microscopy. *J. Cell Sci.* **103**, 857-862.

Martelli, A. M., Gilmour, R. R., Falcieri, E., Manzoli, F. A. and Cocco, L. (1990). Temperature dependant association of DNA polymerase activity with the nuclear matrix. *Exp. Cell Res.* **190**, 227-232.

Mazzotti, G., Rizzoli, R., Galanzi, A., Papa, S., Vitale, M., Falconi, M., Neri, L. M., Zini, N. and Maraldi, N. M. (1990). High-resolution detection of newly-synthesized DNA by anti-bromodeoxyuridine antibodies identifies specific chromatin domains. *J. Histochem. Cytochem.* **38**, 13-22.

Mills, A. D., Blow, J. J., White, J. G., Amos, W. B., Wilcock, D. and Laskey, R. A. (1989). Replication occurs at discrete foci spaced throughout nuclei replicating in vitro. *J. Cell Sci.* **94**, 471-477.

Nakamura, H., Morita, T. and Sato, C. (1986). Structural organisation of replicon domains during DNA synthetic phase in the mammalian nucleus. *Exp. Cell Res.* **165**, 291-297.

Nakayasu, H. and Berezney, R. (1989). Mapping replication sites in the eukaryotic cell nucleus. *J. Cell Biol.* **108**, 1-11.

O'Keefe, R. T., Henderson, S. C. and Spector, D. L. (1992). Dynamic organization of DNA replication in mammalian cell nuclei, spatially and temporally defined replication of chromosome-specific α-satellite sequences. *J. Cell Biol.* **116**, 1095-1110.

Ris, H. (1985). The cytoplasmic filament system in critical point-dried whole mount and plastic-embedded sections. *J. Cell Biol.* **100**, 1474-1487.

Saunders, W. S., Cooke, C. A. and Earnshaw, W. C. (1991). Compartmentalization within the nucleus, discovery of a novel sub-nuclear region. *J. Cell Biol.* **115**, 919-932.

(Received 28 March 1994 - Accepted 2 May 1994)